Synthesis and non-linear optical characterization of novel borinate derivatives of cinnamaldehyde†

Mario Rodríguez,[a] José Luis Maldonado,*[a] Gabriel Ramos-Ortíz,[a] Jean François Lamère,[b] Pascal G. Lacroix,*[b] Norberto Farfán,[c] Ma. Eugenia Ochoa,[d] Rosa Santillan,[d] Marco Antonio Meneses-Nava,[a] Oracio Barbosa-García[a] and Keitaro Nakatani[e]

Received (in Montpellier, France) 14th November 2008, Accepted 25th February 2009
First published as an Advance Article on the web 24th April 2009
DOI: 10.1039/b820435g

Herein is reported the synthesis of three new borinates (**2a–2c**) derived from bidentate imine ligands (**1a–1c**), which were prepared from the corresponding cinnamaldehyde derivatives. All compounds were characterized by MS, IR and NMR spectroscopy. The nonlinear optical (NLO) characterization of these molecules having push–pull properties is included. Second order nonlinearities were evaluated at 1.907 μm by the electric-field-induced second harmonic (EFISH) technique through the $\beta \times \mu$ product, showing a trend for a general increase of the NLO response after boron complexation. For borinate **2c**, which has strong electron-donating and electron-withdrawing groups at opposite ends of the π-backbone, $\beta\mu = 1560 \times 10^{-30}$ D cm^5 esu^{-1}, showing a three-fold increase with respect to the ligand **1c** ($\beta\mu = 542 \times 10^{-30}$ D cm^5 esu^{-1}). Third-order nonlinearities, in solid films, were evaluated employing the third harmonic generation (THG) Maker Fringe technique showing $\chi^{(3)}$ susceptibilities of the order of $\chi^{(3)} \sim 10^{-12}$ esu at the infrared wavelength of 1.2 μm. Compounds with the highest $\chi^{(3)}$ values correspond to those having the largest $\beta\mu$ product: for **1c** $\chi^{(3)} = 1.1 \times 10^{-11}$ esu and for **2c** $\chi^{(3)} = 8.4 \times 10^{-12}$ esu.

Introduction

Organic and organometallic materials with large second-order and third order nonlinear optical (NLO) responses, have attracted considerable research interest owing to their potential use in many opto-electronic and photonic applications, such as data storage, communication, switching, image processing and computing.[1–6] The synthesis of novel dipolar organic compounds with specific optical properties is based on molecules having π-electronic systems which are more mobile than those having σ-electronic systems. Furthermore, the initial electron distribution can also be skewed by substituent effects. On the other hand, boron chemistry has emerged as an interesting area of research because compounds containing tri- or tetra-coordinated boron atoms have found applications in several areas of material sciences,[7–9] medicinal sciences[10] and supramolecular chemistry.[11] The advantage of boron chemistry is the possibility of obtaining stable three- and four-coordinated boron compounds, which has been thoroughly employed in the preparation of supramolecular structures.[12] Further, the three-coordinated boron is isoelectronic and isostructural with a positively charged carbocation, thus, with its p orbital the boron atom is an inherently strong π-electron acceptor[9,12,13] (see Fig. 1(a)). The four-coordinated boron atom has been employed to increase the dipole moment in zwitterionic borates[14] (Fig. 1(b)) or to polarize an aza-π-electronic system by the formation of boronates with stable N→B coordinative

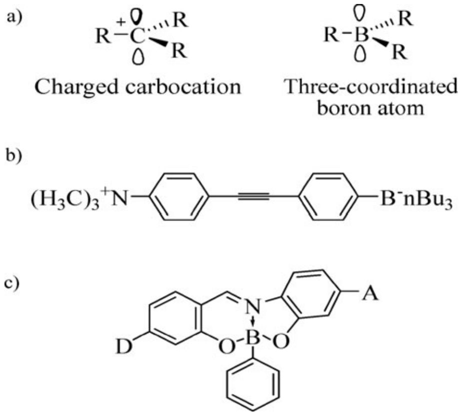

Fig. 1 (a) Comparison of positively charged carbocation and three-coordinated boron atom, (b) zwitterionic borates, and (c) four-coordinated boron atom.

---

[a] Centro de Investigaciones en Óptica A.P. 1-948, 37000, León, Gto, México. E-mail: jlmr@cio.mx
[b] Laboratoire de Chimie de Coordination du CNRS, 205 route de Narbonne, 31077, Toulouse, France
E-mail: Pascal.Lacroix@lcc-toulouse.fr
[c] Facultad de Química, Departamento de Química Orgánica, Universidad Nacional Autónoma de México, México, D.F., 04510, México
[d] Departamento de Química, Centro de Investigación y de Estudios Avanzados del IPN, Apdo. Postal. 14-740, 07000, México D.F., México
[e] Laboratoire de Photophysique et Photochimie Supramoléculaires et Macromoléculaires (UMR 8531 du CNRS), Ecole Normale Supérieure de Cachan, Avenue du Président Wilson, 94235, Cachan, France

† Electronic supplementary information (ESI) available: Cartesian coordinates for calculated structures of **1a–1c** and **2a–2c**. CCDC reference number 705151. For ESI and crystallographic data in CIF or other electronic format see DOI: 10.1039/b820435g

bonds;[15] this has been used in organic synthesis[16] and supramolecular chemistry.[17] Owing to these electronic features, the possibilities for strong NLO response in boron containing chromophores have become naturally addressed.[8,9,18,19] Other optical uses are two-photon absorption and fluorescence,[20,21] two-photon chemosensors,[22] *etc.*

We have previously reported the synthesis and quadratic non-linear optical properties of push–pull boronates, which were prepared by reaction of tridentate ligands derived from salicylideniminophenols with phenylboronic acid[23] (Fig. 1(c)). The electric field induced second harmonic (EFISH) measurements of these boronates showed that the combination of $N(Et)_2$–NO_2 (D–A in Fig. 1(c)) groups, connected to the aza-stilbene backbone, had a $\beta\mu$ (β is the first molecular hyperpolarizability and μ is the dipole moment) value of 451×10^{-30} D cm^5 esu^{-1} while boronates containing the OMe–NO_2 combination had $\beta\mu = 130 \times 10^{-30}$ D cm^{-5} esu^{-1}.

A computational investigation has also suggested that, for a set of D–A substituents (Fig. 1(c)), the NLO response is very dependent on conformational changes around the boron center, a possibility which may lead to further interesting perspectives in the field of molecular switches.[23,24] Further research on different three-coordinated organoboron compounds has been reported,[8b,c,18] where β and γ (the second molecular hyperpolarizability) have been measured between 1 and 50×10^{-30} esu and between 15 and 230×10^{-36} esu, respectively.

In the present work, we report the synthesis of three new borinates (**2a–2c**) from the reaction of diphenylborinic acid and bidentate ligands (**1a–1c**). These series of compounds were synthesized because the introduction of a diphenylborinic acid improves the planarity of the π-skeleton and so, their chemical and optical properties are modified by the formation of a coordinative (N→B) bond. Quadratic ($\beta\mu$) and cubic ($\chi^{(3)}$, third-order electric susceptibility) non-linear optical characterization of **1a–1c** and **2a–2c** molecules having push–pull properties were carried out through EFISH and THG (third harmonic generation) Maker Fringe techniques, respectively.

Experimental

Instrumentation

All starting materials were purchased from Aldrich. Solvents were used without further purification. Melting points were recorded on an Electrothermal 9200 apparatus and are uncorrected. Infrared spectra were measured on a FT-IR Perkin-Elmer GX spectrophotometer using KBr pellets. ^{1}H, ^{11}B and ^{13}C NMR spectra were recorded on a Bruker Avance DPX 300 and Jeol GX 270. Chemical shifts (ppm) are relative to $(CH_3)_4Si$ for ^{1}H and ^{13}C and to $BF_3(OEt_2)$ for ^{11}B. UV-Vis-IR spectra were obtained with a Perkin-Elmer Lambda 900 spectrophotometer. Elemental analyses were carried out on a Thermo Finnigan Flash EA 1112 elemental microanalyzer. Mass spectra, at low resolution, were recorded on a Hewlett Packard 5989A spectrometer using the electron ionization technique at 20 eV. At high resolution, the mass analysis was performed through the Atmospheric Pressure Chemical Ionization (APCI) technique (by using an Agilent G1969A electrospray ionization time of flight spectrometer). X-Ray diffraction studies for single crystals of compound **2d** were performed on a KAPPA CCD diffractometer at 293 K. Solution and refinement: direct method SHELXS-97 for structure solution and SHELXL-97[25] software package for refinement and data output. All the heavier atoms were found by Fourier map difference and refined isotropically. The remaining hydrogen atoms were geometrically modeled. Crystal data are summarized in Table 1.

Table 1 X-Ray crystal data for compound **2d**

Chemical formula	$C_{28}H_{24}BNO$
M_r	401.32
Crystal system	Monoclinic
Space group	$P2_1/c$
a/Å	9.987(2)
b/Å	26.152(5)
c/Å	8.5290(17)
β/°	94.71(3)
V/Å^3	2220.1(8)
Z	4
T/K	293(3)
Refl. collected	5022
Refl. unique	3824
Refl. observed	3824
No. variables	280
Final R [$I > 2\sigma(I)$]	0.0599
Final wR_2	0.1048
GooF	1.074

Synthesis

The bidentate ligands (**1a–1c**) were prepared from the reaction between the appropriate 2-aminophenol and the corresponding cinnamaldehyde derivative (Scheme 1) in methanol at reflux temperature with yields from 75 to 80%. The borinate derivatives (**2a–2c**) were prepared from the reaction of the ligands **1a–1c** with diphenylborinic acid, freshly liberated from the ester complex. These reactions were carried out under reflux in ethyl acetate as solvent for 1–2 h to give the corresponding borinates (**2a–2c**) with yields from 80 to 90%. All compounds (**1a–1c** and **2a–2c**) were soluble in common organic solvents, enabling their optical characterization by EFISH (liquid samples) and THG Maker Fringes (thin film samples) techniques.

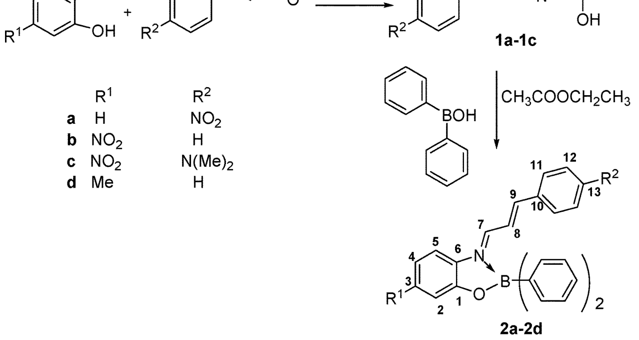

Scheme 1 Synthesis of bidentate ligands (**1a–1c**) and borinates (**2a–2d**).

2-[3-(4-Nitrophenyl)allylideneamino]phenol 1a. The title compound was prepared from 4′-nitro-*trans*-cinnamaldehyde 1.77 g (10 mmol) and *ortho*-aminophenol 1.09 g (10 mmol), to give 2.01 g (7.5 mmol, 75% yield) of **1a**; mp 161–162 °C. *Spectroscopic data*: IR (KBr) ν_{max}: 2916, 2364, 1602 (C=N), 1533, 1483, 1350, 1220, 1198, 972 cm^{-1}. ^{1}H NMR (CDCl$_3$, 300 MHz) δ: 8.53 (1H, dd, J = 5.5 Hz, H-7), 8.28 (2H, d, J = 8.8 Hz, H-12), 7.69 (2H, d, J = 8.8 Hz, H-11), 7.30–7.23 (4H, m, H-8, -9, -5, -3), 7.02 (1H, d, J = 8.2 Hz, H-2), 6.89 (1H, t, J = 7.9 Hz, H-4) ppm. ^{13}C NMR (CDCl$_3$, 75 MHz) δ: 156.7 (C-7), 152.9 (C-1), 148.1 (C-13), 141.9 (C-10), 140.6 (C-8), 135.2 (C-6), 132.7 (C-9), 130.0 (C-3), 128.1 (C-11), 124.4 (C-12), 120.3 (C-4), 115.6 (C-5), 115.5 (C-2) ppm. MS (20 eV) m/z (%): 268 (M$^+$, 51), 267 (67), 251 (45), 222 (19), 221 (100), 204 (6), 146 (9), 120 (18), 108 (9), 93 (5), 80 (7), 65 (5). HRMS calc. m/z for $C_{15}H_{13}N_2O_3$ [M$^+$ + H]$^+$: 269.0962. Found: 269.0929, error 3.08 ppm.

5-Nitro-2-((*E*)-((*E*)-3-phenylallylidene)amino)phenol 1b. The title compound was prepared from *trans*-cinnamaldehyde 1.32 g (10 mmol) and 5-nitro-2-aminophenol 1.54 g (10 mmol), to give 2.14 g (8 mmol, 80% yield) of **1b**; mp 171–172 °C. *Spectroscopic data*: IR (KBr) ν_{max}: 2920, 1608 (C=N), 1539, 1490, 1330, 1222, 1195, 970 cm^{-1}. ^{1}H NMR (CDCl$_3$, 300 MHz) δ: 8.54 (1H, d, J = 8.8 Hz, H-7), 7.85 (1H, d, J = 2.4 Hz, H-2), 7.82 (1H, dd, J = 8.5, 2.4 Hz, H-4), 7.66–7.58 (2H, m, H-11), 7.49–7.44 (3H, m, H-12, 13), 7.36 (1H, d, J = 15.8 Hz, H-8), 7.30 (1H, d, J = 8.5 Hz, H- 5), 7.16 (1H, dd, J = 15.8, 8.8 Hz, H-9) ppm. ^{13}C NMR (CDCl$_3$, 75 MHz) δ: 162.6 (C-7), 152.3 (C-1), 147.6 (C-8), 147.4 (C-3), 141.6 (C-6), 135.1 (C-10), 130.7 (C-13), 129.3 (C-12), 128.1 (C-11), 127.9 (C-9), 116.1 (C-5), 116.0 (C-4), 110.6 (C-2) ppm. MS m/z (%): 268 (M$^+$, 40), 267 (M$^+$ − H, 100), 221 (34), 115 (12). HRMS calc. m/z for $C_{15}H_{13}N_2O_3$ [M$^+$ + H]$^+$: 269.0962. Found: 269.0925, error 1.60 ppm.

2-((*E*)-((*E*)-3-(4-(dimethylamino)phenyl)allylidene)amino)-5-nitrophenol 1c. The title compound was prepared from 4′-dimethylamino-*trans*-cinnamaldehyde 1.54 g (10.0 mmol) and 5-nitro-2-aminophenol 1.75 g (10 mmol), to give 2.86 g (9.1 mmol, 90% yield) of **1c**; mp 188–189 °C. *Spectroscopic data*: IR (KBr) ν_{max}: 3562, 2914, 1605 (C=N), 1566, 1533, 1516, 1380, 1283, 1190, 970 cm^{-1}. ^{1}H NMR (CDCl$_3$, 270 MHz) δ: 8.46 (1H, d, J = 6.2 Hz, H-7), 7.81–7.78 (3H, m, H-9, 5, 2), 7.48 (2H, J = 6.0 Hz, H-12), 7.23 (1H, d, J = 8.8 Hz, H-4), 6.96 (1H, dd, J = 12.0, 6.2 Hz, H-8), 6.72 (2H, d, J = 6.0 Hz, H-11), 3.06 (6H, s, NMe) ppm. ^{13}C NMR (CDCl$_3$, 75 MHz) δ: 163.1 (C-7), 152.3 (C-13), 152.2 (C-1), 149.1 (C-8), 146.8 (C-3), 142.8 (C-6), 130.5 (C-11), 123.2 (C-10), 122.1 (C-9), 116.2 (C-5), 115.9 (C-4), 112.3 (C-12), 110.3 (C-2), 40.5 (NMe) ppm. MS (20 eV) m/z (%): 312 (M$^+$, 12), 311 (M$^+$ − H, 69), 310 (M$^+$ − 2H, 100), 280 (2), 264 (31), 221 (6), 158 (22), 147 (7), 121 (2). HRMS calc. m/z for $C_{17}H_{18}N_3O_3$ [M$^+$ + H]$^+$: 312.1342. Found: 312.1343, error 0.10 ppm.

(*E*)-3-(4-Nitrophenyl)allylidene)-2,3-dihydrobenzo[*d*][1,3,2]-oxazaborole 2a. The title compound was prepared from ligand **1a** 2.68 g (10 mmol) and diphenylborinic acid 1.82 g (10 mmol), to give 3.88 g (9 mmol, 88% yield) of **2a**; mp 190–192 °C. *Spectroscopic data*: IR (KBr) ν_{max}: 2918, 2848, 2358, 1594 (C=N), 1512, 1480, 1340, 1312, 1188, 1148, 1106, 982 cm^{-1}. ^{1}H NMR (CDCl$_3$, 300 MHz) δ: 8.47 (1H, d, J = 9.7 Hz, H-7), 8.18 (1H, d J = 8.7 Hz, H-12), 7.57–7.49 (2H, m, H-*o*,*o*′), 7.46 (1H, d, J = 8.6 Hz, H-2), 7.38 (1H, t, J = 8.5 Hz, H-4), 7.33–7.27 (7H, m, H-*m*,*m*′,*p*,*p*′, H-11, H-9), 7.26 (1H, dd, J = 15.7, 9.7 Hz, H-8), 7.10 (1H, d, J = 8.5 Hz, H-5), 6.88 (1H, t, J = 8.6 Hz, H-3) ppm. ^{13}C NMR (CDCl$_3$, 75 MHz) δ: 161.6 (C-1), 150.1 (C-7), 148.7 (C-13), 145.0 (C-8), 140.6 (C-10), 133.9 (C-3), 132.8 (C-*o*,*o*′), 131.6 (C-6), 128.9 (C-*p*,*p*′), 127.9 (C-*m*,*m*′), 127.4 (C-11), 126.1 (C-9), 124.5 (C-12), 119.0 (C-4), 116.2 (C-5), 114.1 (C-2) ppm. ^{11}B NMR (CDCl$_3$, 96 MHz) δ: 10.0 ($h_{1/2}$ = 480 Hz) ppm. MS (20 eV) m/z (%): 432 (13), 415 (2), 356 (22), 355 (100), 354 (23), 309 (9), 308 (14), 307 (5), 238 (6), 232 (12), 219 (10), 195 (5). HRMS calc. m/z for $C_{27}H_{22}BN_2O_3$ [M$^+$ + H]$^+$: 433.1717. Found: 433.1723, error 2.07 ppm.

6-Nitro-((*E*)-3-phenylallylidene)-2,3-dihydrobenzo[*d*][1,3,2]-oxazaborole 2b. The title compound was prepared from ligand **1b** 2.68 g (10 mmol) and diphenylborinic acid 1.82 g (10 mmol), to give 3.40 g (8 mmol, 78% yield) of **2b**; mp 179–180 °C. *Spectroscopic data*: IR (KBr) ν_{max}: 2925, 2860, 2360, 1590 (C=N), 1505, 1495, 1335, 1310, 1181, 1145, 1106, 982 cm^{-1}. ^{1}H NMR (CDCl$_3$, 300 MHz) δ: 8.56 (1H, d, J = 10.3 Hz, H-7), 7.86 (1H, d, J = 2.2 Hz, H-2), 7.76 (1H, dd, J = 8.8, 2.2 Hz, H-4), 7.54–7.48 (4H, m, H-*o*,*o*′), 7.44 (1H, d, J = 8.8 Hz, H-5), 7.39 (2H, d, J = 15.1 Hz, H-9), 7.36–7.26 (8H, m, H-*m*,*m*′,*p*,*p*′, 11,12,13), 7.22 (1H, dd, J = 15.1, 10.3 Hz, H-8) ppm. ^{13}C NMR (CDCl$_3$, 75 MHz) δ: 161.1 (C-1), 156.3 (C-7), 154.0 (C-8), 150.7 (C-3), 137.1 (C-6), 134.5 (C-10), 133.0 (C-*o*,*o*′), 132.9 (C-9), 129.7 (C-*p*′), 129.5 (C-12), 128.2 (C-*m*,*m*′), 127.7 (C-11), 122.3 (C-13), 114.1 (5), 113.9 (4), 111.0 (C-2) ppm. ^{11}B NMR (CDCl$_3$, 96 MHz) δ: 11.0 ($h_{1/2}$ = 432 Hz) ppm. MS (20 eV) m/z (%): 432 (10), 356 (23), 355 (100), 354 (25), 310 (10), 309 (46), 308 (39), 309 (10), 277 (9), 232 (38), 231 (18), 193 (47), 115 (14), 91 (13). HRMS calc. m/z for $C_{27}H_{22}BN_2O_3$ [M$^+$ + H]$^+$: 433.1717. Found: 433.1718, error 0.001 ppm.

6-Nitro-3-(*E*)-3-(4-dimethylaminophenyl)allylidene)-2,3-dihydrobenzo[*d*][1,3,2]oxazaborole 2c. The title compound was prepared from ligand **1c** 3.11 g (10 mmol) and diphenylborinic acid 1.82 g (10 mmol), to give 4.20 g (8.8 mmol, 88% yield) of **2c**; mp 228–230 °C. *Spectroscopic data*: IR (KBr) ν_{max}: 2916, 1590 (C=N), 1572, 1474, 1438, 1368, 1338, 1322, 1278, 1186 cm^{-1}. ^{1}H NMR (CDCl$_3$, 270 MHz) δ: 8.30 (1H, d, J = 10.8 Hz, H-7), 7.73 (1H, d, J = 2.3 Hz, H-2), 7.64, (1H, dd, J = 8.6, 2.3 Hz, H-4), 7.48 (4H, dd, J = 7.9, 1.8 Hz, H-*o*,*o*′), 7.22-7.31 (7H, m, H-*m*,*m*′,*p*,*p*′, 5), 7.15 (1H, d, J = 15.0 Hz, H-9), 7.13 (2H, d, J = 8.9 Hz, H-11), 6.86 (1H, dd, J = 15.0, 10.8 Hz, H-8), 6.56 (2H, d, J = 8.9 Hz, H-12), 3.07 (3H, s, Me) ppm. ^{13}C NMR (CDCl$_3$, 67 MHz) δ: 159.8 (C-1), 155.4 (C-7), 155.1 (C-8), 153.4 (C-13), 148.8 (C-3), 138.2 (C-6), 132.8 (C-*o*), 132.2 (C-11), 127.5 (C-*m*), 126.9 (C-*p*), 122.4 (C-10), 116.3 (C-9), 113.7 (C-5), 112.2 (C-4), 111.9 (C-12), 109.5 (C-2), 40.1 (C-Me) ppm. MS (20 eV) m/z (%): 475 (61), 474 (24), 399 (28), 398 (100), 397 (26), 240 (17), 237 (12), 236 (58), 210 (23), 158 (11), 134 (11), 78 (12). Anal. Calc. for $C_{29}H_{26}BN_3O_3$: C, 73.28; H, 5.51; N, 8.84. Found: C, 73.11; H, 5.49; N, 8.98%.

6-Methyl-((*E*)-3-phenylallylidene)-2,3-dihydrobenzo[*d*][1,3,2]-oxazaborole 2d. The title compound was prepared from ligand 5-nitro-2-((*E*)-((*E*)-3-phenylallylidene)amino)phenol 2.37 g (10 mmol) and diphenylborinic acid 1.82 g (10 mmol), to give 3.20 g (8 mmol, 82% yield) of **2b**; mp 246–248 °C. *Spectroscopic data*: IR (KBr) ν_{max}: 3068, 3046, 1610, 1584, 1485, 1321, 1299, 1192, 1176, 977, 970 cm^{-1}. ^{1}H NMR ($CDCl_3$, 300 MHz) δ: 8.70 (1H, d, J = 9.4 Hz, H-7), 7.55 (4H, dd, J = 6.5, 2,0 Hz, H-*o*,*o*′), 7.36–7.26 (10H, m, H-*m*,*m*′,*p*,*p*′, 8, 11, 5), 7.21–7.03 (4H, m, H-12, 13, 9), 6.94 (1H, d, J = 7.8 Hz, H-4), 6.60 (1H, d, J = 7 Hz, H-2) ppm. ^{13}C NMR ($CDCl_3$, 67 MHz) δ: 161.8 (C-1), 155.5 (C-7), 149.1 (C-9), 134.8 (C-6, C-10), 132.9 (C-*o*,*o*′), 131.8 (C-13), 131.2 (C-8), 130.4 (C-3), 129.1 (C-*p*,*p*′), 128.5 (C-12), 127.6 (C-m, m′), 126.9 (C-11), 123.8 (C-4), 122.1 (C-5), 113.4 (C-2), 21.5 (Me) ppm. ^{11}B NMR ($CDCl_3$, 96 MHz) δ: 11.0 ($h_{1/2}$ = 371 Hz) ppm. MS (20 eV) *m*/*z* (%): 401 (12), 325 (25), 324 (100), 323 (26), 246 (16), 193 (10), 115 (10) 91 (22). HRMS calc. *m*/*z* for $C_{28}H_{25}BNO$ $[M^{+} + H]^{+}$: 402.2032. Found: 402.2023, error 2.06 ppm.

Optical measurements

Second order. The experimental hyperpolarizabilities (β) were investigated by the electric field induced second harmonic (EFISH) technique.[2,4] The EFISH technique is based on measuring the frequency-doubled light generated in a solution. The $\beta\mu$ values were measured using the wavelength of 1.907 μm generated by the outcoming Stokes-shifted radiation of the Raman scattering in a hydrogen cell (1 m long, 50 bar) pumped with a nanosecond Nd:YAG pulsed (10 Hz) laser operating at 1.064 μm. The centrosymmetry of the solution was broken by dipolar orientation of the chromophores with a high voltage peak (5 kV) synchronized with the laser pulse. The SHG signal was selected through a suitable interference filter, detected by a photomultiplier, and recorded on a Tektronix TDS 620 oscilloscope.

Third order. The THG Maker-Fringes[26] technique measures the $\chi^{(3)}$ coefficient, and consists on the analysis of the oscillations in the THG intensity produced from an active film on a substrate, as a consequence of the variations in the incident angle for the pumping laser beam.[2,4] The molecules were studied in the solid state (solid films) using the guest (molecule)–host (polymer) approach. Ratios of 70 : 30 wt% of polystyrene (PS) and ligands **1a–1c** or borinates **2a–2c**, respectively, were dissolved in chloroform. The solid films were deposited on fused silica substrates (1 mm-thick) by using the spin coating technique. The prepared films had typical thickness between 90 and 160 nm with good optical quality at visible and NIR wavelengths. Sample thickness was measured by using a Dektak 6M profiler. THG Maker-fringes setup is reported elsewhere.[27] The relation of $\chi^{(3)}$ with γ, the second molecular hyperpolarizability, is given by $\langle\gamma\rangle = \chi^{(3)}/L^{4}N_{s}$ where N_s is the density of molecules in the polymer films and $L = (n^2 + 2)/3$ is the correction factor due to local field effects,[28] n being the refractive index.

Theoretical methods

The six derivatives **1a–1c** and **2a–2c** were fully optimized, using the Gaussian-98 program package,[29] within the framework of the density functional theory (DFT) at the B3PW91/6-31G* level. The metric parameters used as starting points for the optimizations were those of the reported structure **2d**. In order to test the reliability of the DFT optimization, the calculations were performed on **2d**, and compared with the actual X-ray geometry. A general tendency for slightly longer bond lengths in the calculated molecule is observed, with a largest deviation of 0.023 Å between C1 and O1. The differences between calculated and experimental angles are less than 1° in all instances. Owing to these similarities, the agreement is satisfactory, which allow the use of the optimized **1a–1c** and **2a–2c** structures to analyze the origin of the NLO response of these chromophores. For the six derivatives, a vibrational analysis was performed at the same level, in order to check the presence of a minimum on the potential energy surface.

The all-valence INDO (intermediate neglect of differential overlap) method,[30] was employed for the calculation of the electronic transitions, in order to analyze the origin of the charge transfer at the atomic level. Calculations were performed using the INDO/1 Hamiltonian incorporated in the commercially available MSI software package ZINDO.[31] The monoexcited configuration interaction (MECI) approximation was employed to describe the excited states. The 100 lowest energy transitions between the 10 highest occupied molecular orbitals and the 10 lowest unoccupied ones were chosen to undergo CI mixing.

Results and discussion

Chemical and structural characterization

The IR spectrum for compounds **1a–1c** shows the C=N stretching band (1602 cm^{-1} for **1a**, 1608 for **1b**, and 1605 cm^{-1} for **1c**). These bands are shifted to higher wavenumbers in comparison to those for borinates **2a–2c** (1594 cm^{-1} for **2a**, 1589 for **2b**, and 1590 cm^{-1} for **2c**), due to the formation of the N→B coordinative bond. The possibility for C=N double bond elongation upon boron complexation and the consequences on the overall charge delocalization will be further discussed within the framework of a computational DFT investigation (*vide infra*).

As an additional evidence of the formation of borinates **2a–2c**, the ^{1}H NMR data show the doublet signal for the azomethine group from 8.46 to 8.54 ppm in the ligands and from 8.30 to 8.56 ppm for the borinates. Moreover, the ^{1}H NMR spectra for borinates **2a–2c** show an ABX system for H-7 (8.47 for **2a**, 8.56 for **2b**, and 8.30 for **2c**), H-8 (7.26 for **2a**, 7.22 for **2b**, and 6.86 for **2c**), and H-9 (7.15 to 7.39 ppm), wherein the coupling constant between H-8 and H-9 (J = 15.0–15.7 Hz) is indicative of a *trans* configuration (J_{trans} = 12 to 18 Hz), which is in agreement with the values reported in the literature.[32] Additionally, the AA′BB′ system in the spectra of compounds **2a** (J_{AB} = 8.7 Hz) and **2c** (J_{AB} = 8.9 Hz) is indicative of *para* substitution in the aromatic ring of the cinnamaldehyde moiety.

The ^{13}C NMR spectrum for compounds **2a–2c** (150.1, 156.3 and 155.4 ppm, respectively) shows a signal for the C=N fragment, which is shifted to lower frequency than the corresponding signals of ligands **1a–1c** (156.7, 162.6 and 163.1 ppm, respectively). This is a consequence of the polarization promoted by the coordinative bond. Other signals, taken as evidence of the formation of borinates **2a–2c**, are C-8 (145.0 for **2a**, 154.0 for **2b**, and 155.1 ppm for **2c**) and C-9 (from 126.1 to 116.3 ppm), which are shifted to higher frequency and lower frequency, respectively. The C-1 signal is shifted to higher frequency ($\Delta\delta_{\max}$ = 9 ppm) due to the formation of the five-membered ring containing the boron atom, which is characteristic for boronates derived from salicylideniminophenols.[33] Unambiguous assignment of the ^{1}H and ^{13}C spectra for all compounds was based on one- and two-dimensional techniques (COSY and HETCOR). Finally the ^{11}B NMR spectra of compounds **2a–2c** show signals with shifts corresponding to the tetrahedral boron atom, 10.0 ppm for **2a**, 10.5 ppm for **2b**, and 11.0 ppm for **2c**.[16]

Compound **2d** (see Scheme 1 and Fig. 2), containing a methyl group, was prepared following the synthetic method reported for the preparation of the borinates **2a–2c** and its X-ray data were used to obtain the skeleton to perform the optimization of structures for **1a–1c** and **2a–2c**. Since it is known that the methyl group helps in the crystallization process for organic molecules, then it was possible to obtain crystals of **2d** through slow evaporation of a mixture of the solvents ethyl acetate and hexane from a saturated solution. The crystallographic data are summarized in Table 1. The X-ray diffraction analysis confirmed the structure of compound **2d**. The coordinative N→B bond with a distance of 1.652(4) Å is larger than that of previously described boronate derivatives of salicilylaminophenols, (1.616(5)) Å.[23] A four-coordinated boron atom is shown in the solid structure with angles around it from 116.4(3) to 99.0(2)°, where the smallest one corresponds to O(1)–B(1)–N(1). In solid state the **2c** structure shows that the azabutadiene N(1)═C(7)–C(8)═C(9) system presents a *trans* arrangement with a torsion angle of 178.4(3)°. The double bond C(8)═C(9) fragment has a *trans* configuration with a torsion angle of 179.6 (3)°, that confirms the ^{1}H NMR observations. The bond distances for the azabutadiene fragment are 1.304(4), 1.422(4), and 1.341(4) Å for N(1)–C(7), C(7)–C(8) and C(8)–C(9), respectively. The N(1)═C(7) bond shows an elongation in its bond distance with respect to the standard value for N═C: 1.27 Å.[34] The central π-backbone is nearly planar with torsion angles of 1.4(5) and 176.6(3)° for the C(5)–C(6)–N(1)–C(7) and C(8)–C(9)–C(10)–C(15) fragments, respectively. This could indicate that the diphenylborinic moiety promotes the planarity of the π-backbone in solid state.

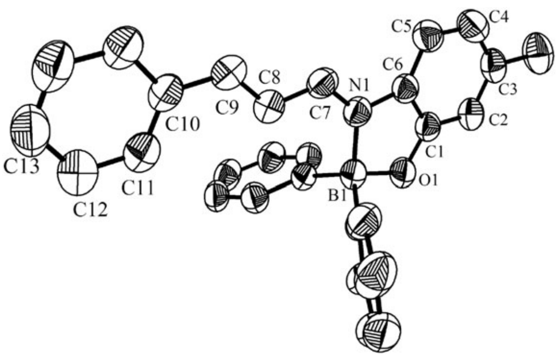

Fig. 2 Molecular view of compound **2d**. The ellipsoids are shown with 50% of probability and hydrogen atoms are omitted for clarity.

In order to provide additional structural characterization for the borinate derivatives, the gas-phase geometries of **1a–1c** and **2a–2c** were fully optimized by DFT, and the X-ray data of **2d** were used to build the starting geometries for the calculations. The main features of the coordination sphere of the boron atom are summarized in Table 2, and these are found to be similar to those of the available crystal structure, which proves the relevance of the optimization process to satisfactorily account for the actual structures of the new borinate species.

A careful examination of the computed data provides additional insights for a modulation of the bond length along the conjugated –C═C–C═N– linkage, upon boron complexation, in full agreement with the spectroscopic studies. The data gathered in Table 3 clearly show a general trend for a slight double bond elongation (and single bond shortening) after boron-nitrogen coordination, allowing a better π-delocalization over the entire molecule.

In order to quantify the NLO capabilities of "push–pull" molecules having a polyenic linker, Marder *et al.*[35,36] have used a geometrical coordinate, the bond length alternation (BLA). BLA is defined as the difference in length between two adjacent carbon–carbon bonds in the polyenic segment. Importantly, there is an optimum BLA value equal to 0.04 Å, which leads to the largest NLO response. In the present case, the BLA values obtained by DFT gas phase optimizations are provided for the –C═C–C═ linkage in Table 3. It is important to point out that in any case, the boron complexation leads to a reduction of BLA, from 0.08–0.07 to 0.06–0.05 Å which strongly suggests better NLO capabilities for the boron containing species.

Optical linear absorption

Fig. 3 shows the absorption spectra of borinate **2c** and its corresponding ligand **1c** in solutions and dispersed in polymer films. The absorption spectra for compounds **2a–2c** show a red shift (about 90 nm) with respect to the absorption for their ligands **1a–1c**, which is characteristic of the introduction of the N→B bond.[23] Table 4 summarizes the data of the optical linear characterization for ligands **1a–1c** and borinates **2a–2c**: wavelengths of maximum absorption ($\lambda_{\max}$), the molar extinction coefficient (ε) in solution, and the absorption coefficient (α) for thin polymer films. In any case, there is a significant red shift upon boron complexation, which may be the key parameter for understanding the origin of the NLO response of the borinate species, as will be discussed in the next section. Additionally, Table 4 provides a comparison between

Table 2 DFT computed data (**2a–2c**) compared to the X-ray available structure (**2d**) for relevant bond lengths and angles

	2a	**2b**	**2c**	**2d**[a]
N–B–O/°	99.1	98.7	98.8	99.0(2)
B–N/Å	1.64	1.64	1.64	1.648(4)
B–O/Å	1.51	1.52	1.52	1.517(4)
B–C/Å	1.62	1.62	1.62	1.615(4)

[a] Data acquired from X-ray diffraction analysis.

Table 3 Structural effects induced by boron complexation, with related BLA parameter (see text), in the polyenic fragment for molecules **1a–1c** and **2a–2c**

	DFT computed bond length/Å			BLA[a]/Å
	–C=C–	=C–C=	–C=N–	(C–C) − (C=C)
1a	1.354	1.437	1.289	0.083
2a	1.358	1.426	1.306	0.068
1b	1.354	1.437	1.290	0.083
2b	1.360	1.422	1.307	0.062
1c	1.360	1.431	1.294	0.071
2c	1.368	1.414	1.311	0.046

[a] "Bond length alternation" structural parameter.

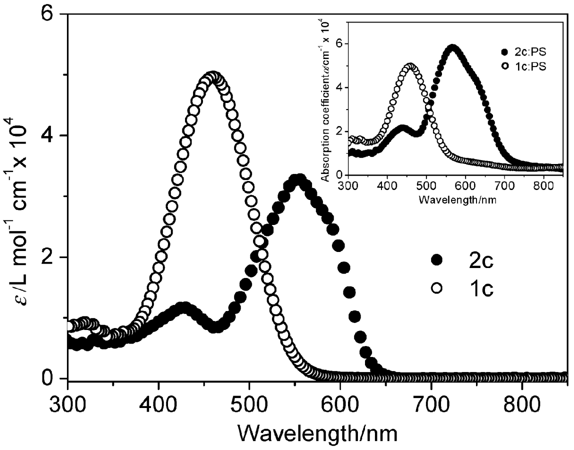

Fig. 3 Optical linear absorption of **1c** and **2c** in chloroform and in polymer films (inset) dispersed into PS (30 : 70 wt%, respectively). Film thickness was 119 and 83 nm, respectively.

experimental and ZINDO calculation. The tendency for a well noted red-shifted transition with the formation of boron complexes is also observed at the theoretical level. For the six derivatives, the transition energies calculated by ZINDO are larger than the experimental ones, with a tendency for a larger difference in the boron complexes (largest energy difference of 4270 cm^{-1} in **2c**). We have previously observed that experimental absorption maxima are significantly red shifted *versus* ZINDO-computed ones in boron-containing chromophores. The difference in energy is frequently found to be in the 2000–5000 cm^{-1} range.[24,37] With respect the discrepancy observed in the present case it is consistent with the previously published data.

For all compounds their photoluminescence (PL) properties were analyzed by pumping with a N_2 laser (337 nm) in a chloroform solution. Under similar experimental conditions, it was possible for **2a**, **1c** and **2c** to measure their PL. Compound **2a** showed the relative strongest emission (red emission). The PL peak wavelengths for **2a**, **1c** and **2c** are at about 647, 667 and 676 nm.

Nonlinear optical (NLO) properties

Second-order nonlinear optical properties. The $\beta\mu$ values for compounds **1a–1c** and **2a–2c** were measured using the EFISH technique; they are shown in Table 5. There was an increase of the ($\beta\mu$) NLO response after boron complexation by a factor equal to 2.8 and 2.9 for systems **a** and **c**, respectively, while system **b** seems to behave differently.

An unexpectedly large $\mu\beta$ value of 1562 × 10^{-30} cm^5 esu^{-1} D was measured for **2c**; the dipole moment has been estimated through indirect dielectric constants measurement[38] for this derivative, and found to be equal to 11 D. This leads to a first hyperpolarizability of 142 × 10^{-30} cm^5 esu^{-1}, which is the highest β value reported for a boronate derivative of salicylideniminophenol ligands.[23,24] However, some diorganotin derivatives[39] and cobalt(II) complexes[40] have also shown similar β value to those of salicylideniminophenol boronates, as well as the pyridine boron complex **3a**, for which $\mu\beta$ = 1560 esu and λ_{max} = 458 nm (Fig. 4).[15] Boronate derivatives of salicylaldehydes and 2-aminophenols have been previously synthesized[23,24] and their first molecular hyperpolarizabilities, measured by the EFISH method, are equal to 25 × 10^{-30} cm^5 esu^{-1} (**4a** of Fig. 4)[23] while **4b**, which is a dimeric species of **4a** had a β of 49 × 10^{-30} cm^5 esu^{-1},[24] *i.e.*, about two times larger than the β of **4a**. Both compounds show values three times smaller than those for **2c** (142 × 10^{-30} cm^5 esu^{-1}), which is reported in this work. Yuan *et al.*[8c,18] have studied other organoboron compounds where β has been measured between 1 and 50 × 10^{-30} esu.

A structural difference between **2c** (–C=C–C=N–) and **4a** (–C=N–) is the elongation of the π-chain connecting the aromatic rings. The β value dependence on π-conjugation length has been investigated in push–pull polyenes,[41] increasing with the length of the chain. Additionally, for compound **2c**, the planarity gained with the use of diphenylborinic acid is another important factor to increase the β value compared

Table 4 Experimental and computed absorption maxima (λ_{max}) and corresponding absorption coefficients for ligands **1a–1c** and borinates **2a–2c**. Films: composites dispersed into PS (30:70 wt% respectively)

			Experimental data			
	Computed (ZINDO) data		Solution		Film	
Compound	λ_{max}/nm	f	λ_{max}/nm	10$^{-4}\varepsilon$/L mol^{-1} cm^{-1}	λ_{max}/nm	10$^{-4}\alpha$/cm^{-1}
1a	373	1.49	388	2.8	397	6.8
2a	432	1.05	492	1.8	493	3.8
1b	372	1.28	388	2.8	394	7.1
2b	415	1.11	474	2.9	475	3.5
1c	397	1.68	460	4.9	458	5.0
2c	448	1.53	552	3.2	566	5.8

Table 5 Experimental quadratic (EFISH at 1907 nm) and cubic (THG at 1200 nm) NLO response for ligands **1a–1c** and borinated materials **2a–2c**

Compound	EFISH ($\mu\beta$)/10^{-30} D cm^5 esu^{-1}	THG ($\chi^{(3)}$)/10^{-12} esu
1a	95	6.4
2a	270	3.7
1b	142	5.7
2b	77	<2.0
1c	541	11.0
2c	1562	8.4

with **4a**[23] and **4b**.[24] We have previously reported that the tetrahedral geometry around the boron atom distorts the structure of the donor–π–acceptor backbone system[23] in salicylideniminophenol ligands. However, the use of a diphenylborinic acid that is bonded only to one aromatic ring of the backbone, does not distort the π-system and instead it contributes to extend its planarity improving the delocalization of the π-electrons.

In order to find a rationale for the origin of the quadratic NLO response in the six different derivatives, it has to be noted that, in π-conjugated molecules, containing donor–acceptor substituents interacting through a π-conjugated bridge, the first molecular hyperpolarizability (β) can ultimately be related to a set of few intense low-lying transitions having charge transfer character, according to the widely used "two-level" (β_{2L}) contribution expressed as follows:[42]

$$\beta_{2L} = \sum_i \frac{3e^2\hbar f_i \Delta\mu_i}{2mE_i^3} \frac{E_i^4}{(E_i^2 - (2\hbar\omega)^2)(E_i^2 - (\hbar\omega)^2)} \qquad (1)$$

In this equation, f_i, $\Delta\mu_i$ and E_i are the oscillator strength, the difference between ground and excited state dipole moment and the energy of the ith transition, respectively ($\hbar\omega$ being the energy of the incident laser beam). The data gathered in Table 6 indicate that, except for **2b**, this approach leads to a NLO response largely dominated by a single transition, in most cases, which encourages us to tentatively relate the NLO response to a single HOMO → LUMO based transition, in the **a** and **c** series (λ_{max} in Fig. 3, and Table 4). Along this line, we can infer that **1a–1c**, **2a**, and **2c** belong to the traditional family of pseudo "push–pull" NLO materials.

Under these assumptions, the effect of the large experimental red shift after boron complexation (104, 86 and 94 nm in **a**, **b**, and **c** series, respectively) can be further quantified by means of eqn (1) for the **a** and **c** series, and found to lead to a β enhancement equal to a factor 2.2 and 4.4, for **2a**, and **2c**, respectively *vs.* that of their related ligand. Before discussing the NLO properties of each **a–c** system in more detail, it may be interesting to point out that this observed red shift is probably a key parameter in the understanding of the behavior of these materials.

The **a** and **c** series are built up from the traditional NLO "push–pull" skeleton, in which a strong acceptor unit (NO_2 in the present case) is connected to a donor counterpart (OH or dimethylamino (DMA) substituents) in **a** and **c** through a nearly one-dimensional π-conjugated spacer. The highly dipolar resulting structures have a "push–pull" electronic character and the main charge transfers ($\Delta\mu$) are directed in the μ direction for such chromophores, as found in **1a** and **1c**. Interestingly, the presence of the additional –B(phenyl)$_2$ group does not lead to any significant change in the charge transfer behavior in **2a** and **2c**. Indeed, a careful examination of the frontier orbitals indicate that –B(phenyl)$_2$ is not involved at both HOMO or LUMO level for these **a** and **c** chromophores (Fig. 5). Nevertheless, the BLA reduction and red shift observed in the presence of –B(phenyl)$_2$ indicate a better charge delocalization over the π-conjugated molecule, together with a lower transition energy (eqn (1)) and finally a global enhancement of the NLO response, as evidenced by the EFISH measurement.

The situation encountered in system **b** seems not to follow the same behavior. Although the BLA reduction and energy shift are observed in the borinated **2b** species, which support the suggestion of β enhancement, the EFISH data undoubtedly indicate a significant reduction of the NLO response. To further discuss this unexpected observation, it is worth reminding that the EFISH experiment requires the poling of the chromophores in their dipole moment direction. Therefore, the experimental optical nonlinearity must be approached through the projection of the hyperpolarizability tensor in the μ direction (β_{vec}). Although it is difficult to determine precisely the actual angle between β and μ, it is generally assumed that $\beta \equiv \beta_{vec}$, in traditional "push–pull" systems (*e.g.* **a** and **c**), a situation which may not be fully applicable in the case of **b**. Indeed, the long π-conjugated (phenyl-CHCHCHN-) backbone has only a NO_2 acceptor group and not a donor substituent, thus lacking the required "push–pull" character of strongly dipolar NLO molecules. Therefore, μ and $\Delta\mu$

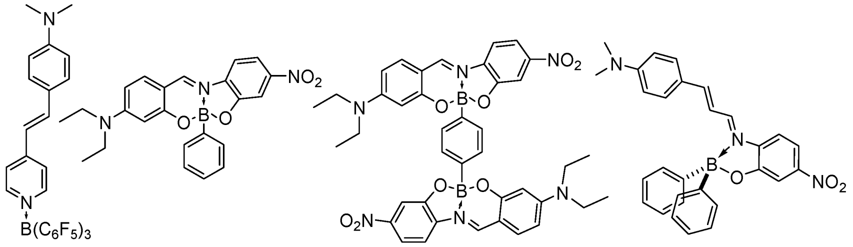

	3a	4a	4b	2c
β (10^{-30} cm^5 esu^{-1})	155	25	49	142

Fig. 4 Structural comparison of borinates **3a**,[15] **4a**,[23] **4b**,[24] and **2c** and their measured β values (see Table 5 for **2c**).

Table 6 Main *i* transition involved in β_{2L} (eqn (1)) calculated by ZINDO, with λ_{max} in nm, weight contribution to β_{2L} (in %), composition of the MECI expansion (see Experimental section), and charge transfer character, for **1a–1c** and **2a–2c**

	λ_{max}/nm	β_{2L}[a] (%)	Composition	Character
1a	373	74	0.830 $\chi_{HOMO\rightarrow LUMO}$	Phenol → nitrophenyl
2a	432	63	0.870 $\chi_{HOMO\rightarrow LUMO}$	Phenol → nitrophenyl
1b	372	69	0.901 $\chi_{HOMO\rightarrow LUMO}$	Phenyl-CHCHCHN → nitrophenyl
2b	415	34	0.955 $\chi_{HOMO\rightarrow LUMO}$	(phi)$_2$B-phenolate → CHCHCHN
1c	397	79	0.799 $\chi_{HOMO\rightarrow LUMO}$	DMAphenyl → nitrophenyl
2c	448	53	0.944 $\chi_{HOMO\rightarrow LUMO}$	(DMAphenyl)-CHCHCHN → CHCHCHN-(nitrophenyl)

[a] $\%_i = \frac{3e^2\hbar f_i\Delta\mu_i}{2mE_i^3}\frac{E_i^4}{(E_i^2-(2\hbar\omega)^2)(E_i^2-(\hbar\omega)^2)}\Big/\sum_i\frac{3e^2\hbar f_i\Delta\mu_i}{2mE_i^3}\frac{E_i^4}{(E_i^2-(2\hbar\omega)^2)(E_i^2-(\hbar\omega)^2)}$

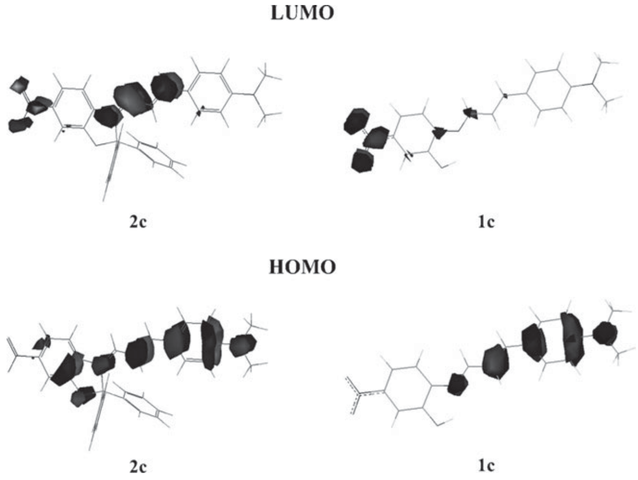

Fig. 5 Comparison of the HOMO (bottom) and LUMO (top) for borinate **2c** (left) and its ligand **1c** (right). Both orbitals were calculated by ZINDO.

(and hence β), may be far from being parallel. At a more fundamental level, we have frequently observed that the β_{2L} description of the optical nonlinearity (eqn (1)) fails in the prediction of the properties, when the donor–acceptor character is not pronounced.[43]

β_{2L} may therefore not be the dominant component to the quadratic NLO response of system **b**. Additionally, the ultimate understanding of the origin of the NLO behavior of **2b** is also hampered by the fact that the HOMO → LUMO based transition provides a crude model, which at best accounts for only 34% of β_{2L} in this case (Table 6). The description of the frontier orbitals reveals that, contrary to the situation encountered in the **a** and **c** series, the –B(phenyl)$_2$ group is engaged at the HOMO level (9% of the electron density). This definitely leads to the conclusion that the origin of the NLO properties of this molecule cannot be regarded within the same picture used for the other derivatives under investigation.

Third-order nonlinear optical properties. The cubic non-linear (macroscopic) response was measured using the third-harmonic generation (THG) Maker-fringes technique[26] exciting at the IR wavelength of 1200 nm. The data values are summarized in Table 5. The THG measurements were performed over thin polymer (polystyrene: PS) films doped with 30 wt% of the borinates **2a–2c** and ligands **1a–1c**. A typical graph obtained from this technique is shown in Fig. 6 for a thin film and its quartz substrate. As the case of quadratic response, the ligand **1c** and its corresponding borinate **2c**, gave the largest values for the $\chi^{(3)}$ susceptibility: $\chi^{(3)} = 1.1 \times 10^{-11}$ esu and $\chi^{(3)} = 8.4 \times 10^{-12}$ esu, respectively. In the borinate **2c**, the $\chi^{(3)}$ value is also influenced by the formation of the N→B coordinative bond, specifically concerning the polarizability of the π-electronic system, this situation could be an important factor for nonlinear optical effects.[44] It is significant to mention that due to the variation of linear absorption of our compounds, there would be a dispersion of the $\chi^{(3)}$ values. Specifically, the absorption coefficient (α/× 10^4 cm^{-1}) for these six samples at 400 nm are: 6.9 and 1.6, 7.0 and 1.5, and 2.5 and 1.6, for **1a** and **2a**, for **1b** and **2b**, and for **1c** and **2c**, respectively, so when using the wavelength of 1200 nm, it is possible to have a slight enhancement for some of them on cubic nonlinearities through three-photon resonance. This could explain the larger $\chi^{(3)}$ values for the ligands than for the borinate compounds (see Table 5).

From the experimental data for $\mu\beta$ and $\chi^{(3)}$ ($\gamma \propto \chi^{(3)}$, see Experimental section) in Table 5, it seems that the effect of boron complexation is completely different for β and γ. Although this tendency seems consistent with the general idea developed by Marder *et al.*,[35] which states that optimizing γ should lead to β cancellation, finding a reliable correlation in the β/γ relationship in these borinated chromophores would deserve further studies.

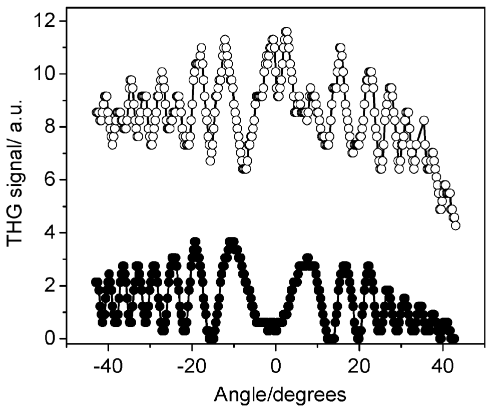

Fig. 6 Third-harmonic light pattern as a function of the incidence angle for a thin polymer film (190 nm) (open circles) doped with 30 wt% of compound **1c**, and for the 1-mm thick fused silica substrate alone (filled circles). The fundamental wavelength is 1200 nm.

Conclusions

Three new borinates **2a–2c** with push–pull character were synthesized in good yield, from the reaction of their corresponding ligands **1a–1c** and diphenylborinic acid. For all compounds, chemical characterizations were performed. ^{1}H, ^{13}C, ^{11}B and bidimensional NMR experiments helped us to confirm the formation of boronates. Additionally, mass spectra and IR spectroscopy were also performed. For the six compounds **1a–1c** and **2a–2c**, second- and third-order optical characterization were measured by EFISH (at 1907 nm) and THG (at 1200 nm) Maker Fringe techniques, respectively. The borinates **2a–2c** and their ligands **1a–1c** showed $\beta\mu$ values between 78 and 1560 $\times$ 10^{-30} cm^{-5} esu^{-1}, and in general an increase in the β value is observed from ligands (**1a** and **1c**) to borinates (**2a** and **2c**) due to the formation of the $N \rightarrow B$ coordinative bond. The largest first hyperpolarizability β is found for the borinate **2c** (142 $\times$ 10^{-30} cm^{5} esu^{-1}), which possess as a donor group $N(CH_3)_2$ and as an acceptor the NO_2 group. In comparison with the values reported previously for boronates, **2c** showed an increment in β that correlates with the elongation of the π-chain arising from the use of the cinnamaldehyde fragment, and also increased planarity of the π-backbone by the use of diphenylborinic acid. With respect to the third-order susceptibility $\chi^{(3)}$, compounds **1c** and **2c**, which have strong electron-donating and electron-withdrawing groups at opposite ends of the π-backbone, had the largest and reasonably high $\chi^{(3)}$ values: 1.1×10^{-11} esu and 8.5×10^{-12} esu, respectively.

Acknowledgements

One of the authors (M. Rodríguez) thanks the ENS Cachan, International Scholarship Program for a grant. This work was partially supported by CONCyTEG (07-04K662-080 A3), CONACyT (55250 and 58783) and UNAM (PAPIIT IN-203207). The authors thank M. L. Rodríguez and G. Uribe for NMR spectra, G. Cuellar for MS spectra and CALMIP (Calcul en Midi Pyrénées-Toulouse, France) for computing facilities. We also thank M. Olmos for his technical assistance, and Dr R. Espinosa-Luna for sample thickness measurements.

References

1 S. R. Forrest and M. E. Thompson, *Chem. Rev.*, 2007, **107**, 923.

2 J. P. Morrall, G. T. Dalton, M. G. Humphrey and M. Samoc, *Adv. Organomet. Chem.*, 2008, **51**, 61.

3 *Nonlinear Optics of Organic Molecules and Polymers*, ed. H. S. Nalwa and S. Miyata, CRC Press, Boca Raton, FL, 1997.

4 *Nonlinear Optical Effects and Materials*, ed. P. Günter, Springer-Verlag, New York, 2000, vol. 72.

5 *Materials for Nonlinear Optics: Chemical Perspectives*, ed. S. R. Marder, J. E. Sohn and G. D. Stucky, ACS Symposium Series 455, American Chemical Society, Washington DC, 1991.

6 S. R. Marder, W. E. Torruellas, M. Blanchard-Desce, V. Ricci, G. I. Stegeman, S. Gilmour, J. L. Brédas, J. Li, G. U. Bublitz and S. G. Boxer, *Science*, 1997, **276**, 1233.

7 C. Branger, M. Lequan, R. M. Lequan, M. Barkazoukas and A. Fort, *J. Mater. Chem.*, 1996, **6**, 555.

8 (*a*) Z. Yuan, N. J. Taylor, T. B. Marder, I. D. Williams, S. K. Kurtz and L.-T. Cheng, *J. Chem. Soc., Chem. Commun.*, 1990, 1489; (*b*) Z. Yuan, N. J. Taylor, R. Ramachandran and T. B. Marder, *Appl. Organomet. Chem.*, 1996, **10**, 305; (*c*) Z. Yuan, J. C. Collings, N. J. Taylor, T. B. Marder, C. Jardin and J.-F. Halet, *J. Solid State Chem.*, 2000, **154**, 5.

9 (*a*) C. D. Entwistle and T. B. Marder, *Angew. Chem., Int. Ed.*, 2002, **41**, 2927; (*b*) C. D. Entwistle and T. B. Marder, *Chem. Mater.*, 2004, **16**, 4574.

10 M. F. Hawthorne and M. W. Lee, *J. Neurooncol.*, 2003, **62**, 33.

11 (*a*) N. Farfán, H. Höpfl, V. Barba, M. E. Ochoa, R. Santillan, E. Gómez and A. Gutiérrez, *J. Organomet. Chem.*, 1990, **581**, 70; (*b*) N. Iwasawa and H. Takahagi, *J. Am. Chem. Soc.*, 2007, **129**, 7754.

12 V. Barba, R. Villamil, R. Luna, C. Godoy-Alcantar, H. Höpfl, H. Beltran, L. S. Zamudio, R. Santillan and N. Farfán, *Inorg. Chem.*, 2006, **45**, 2553.

13 (*a*) N. Matsumi, K. Naka and Y. Chujo, *J. Am. Chem. Soc.*, 1998, **120**, 5112; (*b*) N. Matsumi, T. Umeyama and Y. Chujo, *Macromolecules*, 2001, **34**, 3510.

14 (*a*) C. Lambert, S. Stadler, G. Bourhill and C. Bräuchle, *Angew. Chem.*, 1996, **108**, 710; (*b*) C. Lambert, S. Stadler, G. Bourhill and C. Bräuchle, *Angew. Chem., Int. Ed. Engl.*, 1996, **35**, 644; (*c*) K. C. Ching, M. Lequan, R. M. Lequan, A. Grisard and D. Markovitsi, *J. Chem. Soc., Faraday Trans.*, 1991, **87**, 2225.

15 M. J. G. Lesley, A. Woodward, N. J. Taylor, T. B. Marder, I. Cazenobe, I. Ledoux, J. Zyss, A. Thornton, D. W. Bruce and A. K. Kakkar, *Chem. Mater.*, 1998, **10**, 1355.

16 (*a*) V. Barba, D. Cuahutle, R. Santillan and N. Farfán, *Can. J. Chem.*, 2001, **79**, 1229; (*b*) M. Rodríguez, M. E. Ochoa, R. Santillán, N. Farfán and V. Barba, *J. Organomet. Chem.*, 2005, **690**, 2975; (*c*) M. Rodríguez, M. E. Ochoa, C. Rodríguez, R. Santillán, V. Barba and N. Farfán, *J. Organomet. Chem.*, 2007, **692**, 2425.

17 (*a*) H. Höpfl, M. Sánchez, N. Farfán and V. Barba, *Can. J. Chem.*, 1998, **76**, 1352–1360; (*b*) C. Ikeda and T. Nabeshima, *Chem. Commun.*, 2008, 721.

18 (*a*) Z. Yuan, C. D. Entwistle, J. C. Collings, D. Albesa-Jové, A. S. Batsanov, J. A. K. Howard, N. J. Taylor, H. M. Kaiser, D. E. Kaufmann, S.-Y. Poon, W.-Y. Wong, C. Jardin, S. Fathallah, A. Boucekkine, J.-F. Halet and T. B. Marder, *Chem.–Eur. J.*, 2006, **12**, 2758; (*b*) Z. Yuan, N. J. Taylor, Y. Sun, T. B. Marder, I. D. Williams and L.-T. Cheng, *J. Organomet. Chem.*, 1993, **449**, 27.

19 (*a*) M. Lequan, R. M. Lequan, K. Chane-Ching, A.-C. Callier, M. Barzoukas and A. Fort, *Adv. Mater. Opt. Electr.*, 1992, **1**, 243; (*b*) C. Branger, M. Lequan, R. M. Lequan, M. Large and F. Kajzar, *Chem. Phys. Lett.*, 1997, **272**, 265.

20 (*a*) M. Charlot, L. Porrès, C. D. Entwistle, A. Beeby, T. B. Marder and M. Blanchard-Desce, *Phys. Chem. Chem. Phys.*, 2005, **7**, 600; (*b*) J. C. Collings, S.-Y. Poon, C. Le Droumaguet, M. Charlot, C. Katan, L. O. Palsson, A. Beeby, J. A. Mosely, H. M. Kaiser, D. E. Kaufmann, W.-Y. Wong, M. Blanchard-Desce and T. B. Marder, *Chem.–Eur. J.*, 2009, **15**, 198.

21 (*a*) Z.-Q. Liu, Q. Fang, D. Wang, G. Xue, W.-T. Yu, Z.-S. Shao and M. H. Jiang, *Chem. Commun.*, 2002, 2900; (*b*) Z.-Q. Liu, Q. Fang, D. Wang, D.-X. Cao, G. Xue, W.-T. Yu and H. Lei, *Chem.–Eur. J.*, 2003, **9**, 5074; (*c*) D. X. Cao, Z.-Q. Liu, Q. Fang, G. B. Xu, G. Xue, G. Q. Liu and W. T. Yu, *J. Organomet. Chem.*, 2004, **689**, 2201.

22 Z.-Q. Liu, M. Shi, F.-Y. Li, Q. Fang, Z. H. Chen, T. Yi and C. H. Huang, *Org. Lett.*, 2005, **7**, 5481.

23 H. Reyes, B. M. Muñoz, N. Farfán, R. Santillan, S. Rojas-Lima, P. G. Lacroix and K. Nakatani, *J. Mater. Chem.*, 2002, **12**, 2898.

24 J. F. Lamère, P. G. Lacroix, N. Farfán, J. M. Rivera, R. Santillan and K. Nakatani, *J. Mater. Chem.*, 2006, **16**, 2913.

25 G. M. Sheldrick, *SHEXL-97, Program for Crystal Structure Solution*, University of Göttingen, Germany, 1997.

26 F. Kajzar, J. Messier and C. Rosilio, *J. Appl. Phys.*, 1986, **60**, 3040.

27 (*a*) G. Ramos-Ortiz, J. L. Maldonado, M. A. Meneses-Nava, O. Barbosa-García, M. Olmos-López and M. Cha, *Opt. Mater.*, 2007, **29**, 636; (*b*) G. Ramos-Ortiz, S. Romero, J. L. Maldonado, O. Barbosa-García, M. A. Meneses-Nava, M. Romero and N. Farfán, *Rev. Mex. Fís.*, 2006, **52**, 527.

28 I. R. Whittall, A. M. McDonagh, M. G. Humphrey and M. Samoc, *Adv. Organomet. Chem.*, 1999, **43**, 349.

29 M. J. Frisch, G. W. Trucks, H. B. Schlegel, G. E. Scuseria, M. A. Robb, J. R. Cheeseman, V. G. Zakrzewski, J. A. Montgomery, Jr., R. E. Stratmann, J. C. Burant,

S. Dapprich, J. M. Millam, A. D. Daniels, K. N. Kudin, M. C. Strain, O. Farkas, J. Tomasi, V. Barone, M. Cossi, R. Cammi, B. Mennucci, C. Pomelli, C. Adamo, S. Clifford, J. Ochterski, G. A. Petersson, P. Y. Ayala, Q. Cui, K. Morokuma, D. K. Malick, A. D. Rabuck, K. Raghavachari, J. B. Foresman, J. Cioslowski, J. V. Ortiz, A. G. Baboul, B. B. Stefanov, G. Liu, A. Liashenko, P. Piskorz, I. Komaromi, R. Gomperts, R. L. Martin, D. J. Fox, T. Keith, M. A. Al-Laham, C. Y. Peng, A. Nanayakkara, C. Gonzalez, M. Challacombe, P. M. W. Gill, B. G. Johnson, W. Chen, M. W. Wong, J. L. Andres, M. Head-Gordon, E. S. Replogle and J. A. Pople, *GAUSSIAN 98 (Revision A.9)*, Gaussian, Inc., Pittsburgh, PA, 1998.

30 (*a*) M. C. Zerner, G. H. Loew, R. F. Kirchener and U. Mueller-Westerhoff, *J. Am. Chem. Soc.*, 1980, **102**, 589; (*b*) W. P. Anderson, W. D. Edwards and M. C. Zerner, *Inorg. Chem.*, 1986, **25**, 2728.

31 *ZINDO, release 96.0*, Molecular Simulations Inc., Cambridge, UK, 1996.

32 H. Günther, *NMR spectroscopy, Basic Principles, Concepts and Applications in Chemistry*, Wiley, New York, second edn, 1995, pp. 519–521.

33 V. Barba, J. Vázquez, F. López, R. Santillan and N. Farfán, *J. Organomet. Chem.*, 2005, **690**, 2351.

34 F. H. Allen, O. Kennard, D. G. Watson, L. Brammer, A. G. Orpen and R. Taylor, Typical distances: Organic Compounds, in *International Tables for Crystallography*, Kynoch Press, Birmingham, 1992.

35 (*a*) C. B. Gorman and S. R. Marder, *Proc. Natl. Acad. Sci. USA*, 1993, **90**, 11297; (*b*) S. R. Marder, C. B. Gorman, F. Meyers, J. W. Perry, G. Bourhill, J. L. Brédas and B. M. Pierce, *Science*, 1994, **265**, 632.

36 F. Meyers, S. R. Marder, B. M. Pierce and J. L. Brédas, *J. Am. Chem. Soc.*, 1994, **116**, 10703.

37 H. Reyes, J. M. Rivera, N. Farfán, R. Santillan, P. G. Lacroix, C. Lepetit and K. Nakatani, *J. Organomet. Chem.*, 2005, **690**, 3737.

38 (*a*) Y.-J. Zhu, A.-J. Qin, L.-M. Fu, X.-C. Ai, Z.-X. Guo, J.-P. Zhang and C. Ye, *J. Mater. Chem.*, 2007, **17**, 2101; (*b*) E. A. Guggenheim, *Trans. Faraday Soc.*, 1949, **45**, 714.

39 H. Reyes, C. García, N. Farfán, R. Santillan, P. G. Lacroix, C. Lepetit and K. Nakatani, *J. Organomet. Chem.*, 2004, **689**, 2303.

40 P. G. Lacroix, F. Averseng, I. Malfant and K. Nakatani, *Inorg. Chim. Acta*, 2004, **357**, 3825.

41 Ch. Bosshard, K. Sutter, Ph. Prêtre, J. Hulliger, M. Flörsheimer, P. Kaatz and P. Günter, *Organic Nonlinear Optical Materials*, Gordon and Breach Publishers, Singapore, 1995, pp. 9–10.

42 (*a*) J. L. Oudar, *J. Chem. Phys.*, 1977, **67**, 446–458; (*b*) J. L. Oudar and J. Chemla, *J. Chem. Phys.*, 1977, **66**, 2664.

43 (*a*) J. F. Lamère, I. Sasaki, P. G. Lacroix and K. Nakatani, *New J. Chem.*, 2006, **30**, 921; (*b*) J. P. Costes, J. F. Lamère, C. Lepetit, P. G. Lacroix and F. Dahan, *Inorg. Chem.*, 2005, **44**, 1973; (*c*) C. Lepetit, P. G. Lacroix, V. Peyrou, C. Saccavini and R. Chauvin, *J. Comput. Methods Sci. Eng.*, 2004, **4**, 569.

44 B. M. Muñoz, R. Santillan, M. Rodríguez, J. M. Méndez, M. Romero, N. Farfán, P. G. Lacroix, K. Nakatani, G. Ramos-Ortíz and J. L. Maldonado, *J. Organomet. Chem.*, 2008, **693**, 1321.